

Reliability of complete gravitational waveform models for compact binary coalescences

Frank Ohme,¹ Mark Hannam,² and Sascha Husa³

¹*Max-Planck-Institut für Gravitationsphysik, Am Mühlenberg 1, 14475 Potsdam, Germany*

²*School of Physics and Astronomy, Cardiff University, Cardiff, CF24 3AA, United Kingdom*

³*Departament de Física, Universitat de les Illes Balears, Cra. Valldemossa Km. 7.5, Palma de Mallorca, E-07122 Spain*

(Dated: July 7, 2011)

Accurate knowledge of the gravitational-wave signal from inspiraling compact binaries is essential to detect these signatures in the data from gravitational-wave interferometers. With recent advances in post-Newtonian (PN) theory and numerical relativity (NR) it has become possible to construct inspiral-merger-ringdown waveforms by combining both descriptions into one complete *hybrid* signal. It is important to estimate the error of such waveforms and assess their reliability for detection and parameter estimation in different points of the physical parameter space. Previous studies have identified the PN contribution as the dominant source of error, which can be reduced by incorporating longer NR simulations. There are two outstanding issues that make it difficult to determine the minimum simulation length necessary to produce suitably accurate hybrids for GW astronomy applications: (1) the relevant criteria for a GW search is the mismatch between the true waveform and a set of model waveforms, optimized over all waveforms in the model, but for discrete hybrid waveforms this optimization is not possible. (2) these calculations require that numerical waveforms already exist, while ideally we would like to know the necessary NR waveform length *before* performing the simulation. In this paper we overcome both of these difficulties by developing a general procedure that allows us to estimate hybrid mismatch errors *without* numerical data, and to optimize these mismatches over all physical parameters. Using this procedure we find that, contrary to some earlier studies, ~ 10 NR orbits before merger allow for the construction of waveform families that are accurate enough for detection in a broad range of parameters, only excluding highly spinning, unequal-mass systems. Nonspinning systems, even with high mass-ratio ($\gtrsim 20$) are well modeled for astrophysically reasonable component masses. In addition, the parameter bias is only of the order of 1% for total mass and symmetric mass-ratio and less than 0.1 for the dimensionless spin magnitude. We take the view that similar NR waveform lengths will remain the state of the art in the Advanced detector era, and begin to assess the limits of the science that can be done with them.

PACS numbers: 04.30.Db, 04.25.D-, 04.25.Nx

I. INTRODUCTION

A network of gravitational wave (GW) detectors is preparing to achieve a remarkable scientific goal: the first direct detection of GWs. This will not only test the predictions from Einstein’s general theory of relativity, it will also open a new window to the universe, revealing details of the population, composition and formation history of various astrophysical objects [1]. One particularly interesting and promising source of detectable GWs is the inspiral, merger and ringdown of compact objects, such as black holes or neutron stars.

An important contribution to the effort of detecting the signature of coalescing compact binaries in the noise-dominated spectrum of a GW interferometer is the accurate modeling of the expected signals. Only with an entire family of these theoretically predicted template signals is it possible to filter large amounts of data taken from the interferometers. In a “matched filter” search (see e.g. [2]), these data are convolved with the model signals and if the agreement exceeds some pre-defined threshold one claims detection and further exploits theoretical predictions to estimate physical parameters of the binary system, such as component masses and spins.

In the case of a binary black hole (BBH) with comparable masses, at least two different approaches are needed to describe the full motion and radiated GW content from the system. Post-Newtonian (PN) theory is an asymptotic weak field approximation that treats black holes as point particles with a relative velocity v that is small with respect to the speed of

light c (for details, see e.g., [3] and reference therein). The standard PN formulation is based on expanding the relevant quantities (such as energy and GW flux) in terms of the small parameter v/c . Depending on the details of the expansion, resummation and integration of the resulting differential equations, different waveform models for the early inspiral are known, commonly denoted by TaylorT n (with $n = 1, \dots, 4$) [3–8], TaylorF2 [9–12] and TaylorEt [13, 14]. A further inspiral waveform family is obtained by mapping the two body problem to an effective one body (EOB) system with the appropriate potential [5, 15–17].

All these analytical approximations break down in the strong gravity regime, and one has to perform computationally expensive numerical calculations in full general relativity to describe the complete dynamics. Since 2005 [18–20] stable numerical-relativity (NR) simulations of a few orbits plus merger and ringdown to a final Kerr black hole have become a standard tool to consistently predict the last stages of a BBH coalescence [21]. The exploration of the whole parameter space, however, has just begun and, for instance, long simulations of systems with mass-ratios higher than $q = m_2/m_1 \sim 5$ are still exceptionally time-consuming. For current overviews of the field see [22–25].

An obvious goal is to combine PN and NR results to produce “complete” waveform models. Such signals contain physical information up to frequencies higher than the pure PN templates, which becomes increasingly important when the total mass of the system increases. According to re-

cent studies, binary neutron stars as well as mixed black hole/neutron star binaries are captured well by point-particle PN templates [26, 27] assuming the current and anticipated performance of the Laser Interferometer Gravitational-wave Observatory (LIGO) [28]. We therefore focus on complete waveform models for BBH coalescences in this paper. By including systems with small total masses in our analysis, however, we effectively consider a broad range of possible compact binary systems.

Several approaches have already been suggested to analytically build template families that include all the stages that the BBH undergoes. The EOB family has been refined by adding extra parameters that cannot be determined by PN calculations but are fixed by calibrating them to highly accurate NR data. This combination of EOB and NR information yields a description of the entire coalescence process in the time domain [29–36], often referred to as EOBNR. A different time-domain description based on standard PN expansions was presented in [37] as a step towards modeling generic spin configurations. In this paper, we consider the direct matching of standard PN waveform models to NR data. In this approach, PN data are used up to some point in time or frequency and NR results are then taken to describe the remaining part of the waveform. A phenomenological fitting of these “hybrid” waveforms can then be performed to obtain an analytical closed formula (in the frequency domain) which interpolates between the physical parameters of the hybrids [38–41].

All these procedures are subject to ambiguities and errors that limit the applicability of the final waveforms. The major source of uncertainty is the long PN inspiral part of the waveform, as previous studies have shown [41–44]; and we continue the effort to estimate modeling errors on this basis here. In a previous paper [42] we started addressing the important question of how long numerical waveforms have to be in order to fulfill the accuracy requirements for a PN/NR hybridization. Our analysis of nonspinning binaries with mass-ratio $q \in [1, 4]$ and equal-mass binaries with spins (anti-)aligned to the orbital angular momentum (with $\chi_i = S_i/m_2^2 \leq 0.5$) lead to the conclusion that NR simulations of such systems should cover 5 to 10 orbits to be used in hybrids that satisfy the minimal accuracy requirement for signal detection. For larger mass-ratios and larger spins, our results suggested that far longer numerical waveforms were required.

However, that study was limited due to the following restriction: The efficacy of a model in a search is determined by the best match between the true waveform and *any other waveform* in the search model. This best match (called the “fitting factor”) should be calculated by maximizing the match over all of the physical parameters of the model. With access to hybrids from only discrete points in the parameter space, we were only able to maximize the match over the total mass of the binary, and so our results were a (possibly very) conservative estimate of waveform length requirements.

Even stronger requirements were presented in a number of other studies, where *no* maximization was performed at all (except over the initial phase and time-of-arrival of the signal), with the intention of determining the waveform length requirements not just for detection, but also for parameter es-

timization. With these more stringent requirements, MacDonald *et al.* [43] as well as Boyle [44], concluded that NR waveforms generally have to be *much longer* than currently possible to produce hybrids sufficiently accurate for both detection and parameter estimation. In addition, Damour *et al.* [45] presented a detailed comparison of one phenomenological waveform model [40] and a recent member of the EOBNR family [33]. As part of their approach they find that in particular systems with higher mass-ratio ($q \gtrsim 10$) can be combined accurately with a standard PN approximant in the frequency domain only if the NR waveform contains *hundreds* of orbits.

In this paper, we study hybrid accuracy and NR waveform length requirements in the context of *fully optimized mismatches*, i.e., fitting factors. To do this, we first show that it is possible to estimate the hybrid mismatch *without* full numerical waveforms. This is because to a good approximation we need only integrated quantities from the numerical waveforms (for example, their total power), and these bulk quantities can be calculated with sufficient accuracy from phenomenological models; the uncertainties in the fine details of those models do not affect these calculations. Furthermore, it is possible to generalize this procedure, to allow us to optimize the mismatch with respect to physical parameters, and to then calculate the fitting factor that is necessary to make estimates of NR waveform length requirements that are meaningful for GW searches. By looking at the parameter bias between the best-match waveform and the target signal, we also gain some insight into the parameter estimation errors due to the uncertainties in the waveform modeling process.

In the following sections, we will develop this procedure step by step. After introducing the mismatch as our data analysis-motivated definition of error (Sec. II), we show in Sec. III that the mismatch between two hybrids can be partially estimated with knowledge of only the relative power between the NR and PN parts of the signal. In Sec. IV we include the possible dephasing between the NR parts of two waveforms, which completes our procedure for making an accurate estimate of the mismatch. (This is similar to the procedure presented by [44]). Along the way we compare with previous results in the literature, showing that we fully agree on non-optimized mismatch errors.

When we finally optimize these mismatches with respect to physical parameters in Sec. V, we find that the corresponding errors for waveform families are much smaller than assumed so far. In particular, NR simulations that cover ~ 10 orbits are probably acceptable for most astrophysical applications during the Advanced detector era. This includes nonspinning binaries (for which significant improvements in PN approximants are less likely in the next five years), where we explicitly show that this relatively small number of NR orbits is sufficient up to at least $q = 10$, and with astrophysically reasonable restrictions even for $q = 20$ and above. We also adopt the view that, since typical simulations will be of comparable lengths over the next five years, our focus here and in future work should not be on prescribing ideal (and unrealistic) waveform lengths, but on determining the limits of the science that we can do with them.

II. PRELIMINARY CONSIDERATIONS

We shall address the question of accuracy of BBH hybrid waveforms in the following sense. Let

$$h = h_+ - ih_\times \quad (1)$$

be the complex GW strain that combines the plus and cross polarization of the GW as the real and imaginary part, respectively. It is constructed from its PN description h_{PN} and the NR part h_{NR} . We assume that the transition from h_{PN} to h_{NR} is enforced at a single frequency,

$$\tilde{h}(f) = \begin{cases} \tilde{h}_{\text{PN}}(f), & \text{for } f \leq f_m \\ \tilde{h}_{\text{NR}}(f), & \text{for } f > f_m \end{cases}, \quad (2)$$

where \tilde{h} denotes the Fourier transform of h and f_m is the matching frequency. Such a procedure can be employed in a direct Fourier-domain construction of the hybrid [41], but it is also approximately true for time-domain hybrid constructions. In the latter case, the transition is carried out at a time t_m , where the instantaneous frequency is $\omega(t_m) = \frac{d \arg h}{dt} = 2\pi f_m$. Then, for (2) to be true, we have to assume that

1. the transition frequency in the Fourier-domain is equal to the instantaneous matching frequency calculated in the time-domain;
2. the signal at times $t < t_m$ only significantly affects the Fourier-domain for $f < f_m$ and $t > t_m$ correspondingly determines the wave for $f > f_m$.

These assumptions are not trivial since the Fourier-integral is a ‘‘global’’ transformation. However, it was shown that assuming such a stationarity is reasonable in a regime where both PN and NR are valid [41] and time- and frequency-domain construction methods lead to very similar results [42].

The final hybrid waveform is subject to several errors, and we account for these errors here simply by the fact that one could have taken slightly different ingredients h_{PN} and h_{NR} for the same physical scenario. These could be different post-Newtonian approximants and numerical data from different codes or different resolutions. Denoting the different waveform models by h_1 and h_2 , we calculate the mismatch

$$\mathcal{M} = 1 - \mathcal{O}(h_1, h_2) = 1 - \frac{\langle h_1, h_2 \rangle}{\|h_1\| \|h_2\|} \quad (3)$$

$$= 1 - \max_{\phi_0, t_0} \left[4 \operatorname{Re} \int_{f_1}^{f_2} \frac{\tilde{h}_1(f) \tilde{h}_2^*(f)}{S_n(f)} \frac{df}{\|h_1\| \|h_2\|} \right], \quad (4)$$

where ϕ_0 and t_0 are relative phase and time shifts between the waveforms and $\|h\|^2 = \langle h, h \rangle$. S_n is the noise spectral density of the assumed detector, * indicates the complex conjugation and (f_1, f_2) is a suitable integration range. \mathcal{O} is called the overlap of the two waveforms. Throughout this paper, we will follow the choices of our preceding work [42], i.e., $f_1 = 20\text{Hz}$ and S_n is given by the analytic fit of the design sensitivity of Advanced LIGO [39]. The upper integration bound f_2 is given by our waveform model, and we use $f_2 = 0.15/M$, although

the results do not depend sensitively on this value (M is the total mass of the binary).

Broadly speaking, the mismatch indicates how ‘‘close’’ h_1 and h_2 are. Smaller values for \mathcal{M} represent smaller errors in the waveform model, given that h_1 and h_2 are approximations of the same signal. Direct conclusions can be drawn from calculating the mismatch: If \mathcal{M} is less than some threshold, we regard the final hybrid as *accurate enough* for the purpose in question. For a maximum loss of 10% of the signals in the detection process, we can accept a mismatch of $\approx 3\%$, disregarding the addition from a discrete template spacing. If we account for the latter, one may decrease the accepted mismatch in the waveform modeling to 1.5% (see a similar discussion in [42]) or even 0.5% as suggested in [46].

A generally more stringent requirement is that the uncertainty we have in the modeling is *indistinguishable* by the detector. Such a statement is obviously dependent on how ‘‘loud’’ the signal is in the detector. As discussed in [46] and further detailed in [45, 47] we can write the indistinguishability criterion as

$$\|h_1 - h_2\|^2 < \varepsilon^2, \quad (5)$$

where the waveforms are optimally aligned in the sense of (4) and ε parametrizes the effective noise-increase due to model uncertainties. The minimal requirement for h_1 and h_2 to be indistinguishable is $\varepsilon = 1$, although [45] argues that $\varepsilon \sim 1/2$ and probably less are more reasonable thresholds. Manipulating (5) under the assumption of equal norms leads to the equivalent inequality (see the calculation in [48])

$$\mathcal{M} < \frac{1}{2\rho_{\text{eff}}^2}, \quad (6)$$

where $\rho_{\text{eff}} = \|h\|/\varepsilon$ is the effective signal-to-noise ratio (SNR) of the signal.

When we later calculate \mathcal{M} as a measure of the error in hybrid waveforms, we can set various thresholds based on $\mathcal{M} < \mathcal{M}_{\text{max}}$ or Eq. (6) to evaluate the reliability of current models. A potentially very useful application is then to conclude which matching frequency is needed (i.e., how long do the numerical waveforms have to be) to ensure the desired accuracy.

III. A FIRST APPROXIMATION TO THE HYBRID MISMATCH

Before we calculate mismatches for many different scenarios, we establish a few more assumptions to gain some insights on the structure of Eq. (4). These will allow us to propose an approximation to the mismatch between two hybrid waveforms that can be calculated *without* the need for any NR data.

In addition to (2), we further assume:

3. Following [21, 41] we regard the error on the NR side as small, negligible compared to the uncertainties PN introduces up to currently practical matching frequencies.

4. Independent of the PN approximant that is used, the norm of the waveforms are to high accuracy the same (i.e., only the phase is affected). This is reasonable to take as a good approximation, because the amplitude description in PN is usually formulated as a function of the orbital frequency [49–51] (which we again identify with the content on the Fourier side as well) and the mismatch is much more sensitive to phase differences than to amplitude discrepancies.

With these assumptions, we can find an instructive lower bound on \mathcal{M} :

$$\begin{aligned} \mathcal{M} &= 1 - \frac{4}{\|h\|^2} \max_{\phi_0, t_0} \left[\text{Re} \int_{f_1}^{f_m} \frac{\tilde{h}_1 \tilde{h}_2^*}{S_n} df + \int_{f_m}^{f_2} \frac{|\tilde{h}|^2}{S_n} df \right] \\ &\geq 1 - \frac{\langle h_1, h_2 \rangle}{\|h\|_{(f_1, f_m)}^2} \frac{\|h\|_{(f_1, f_m)}^2}{\|h\|^2} - \frac{\|h\|_{(f_m, f_2)}^2}{\|h\|^2} \\ &= \frac{\|h\|_{(f_1, f_m)}^2}{\|h\|^2} \mathcal{M}_{\text{PN}}. \end{aligned} \quad (7)$$

Here we introduced the notation $\|h\|_{(a,b)}^2$ to specify the integration range. \mathcal{M}_{PN} is the mismatch of the PN part only, restricted to $f < f_m$. In the first line of (7) we use the fact that the amplitudes agree (in fact, we do not require point-wise agreement, only the norm is assumed to be the same) and that $h_1 = h_2$ for $f > f_m$. The second line is a lower estimate because the maximization was originally carried out by shifting the entire waveforms relative to each other, whereas now we allow the maximization over the PN part alone. The final step involves the obvious relation $\|h\|^2 = \|h\|_{(f_1, f_2)}^2 = \|h\|_{(f_1, f_m)}^2 + \|h\|_{(f_m, f_2)}^2$.

Let us emphasize that all numerical tests we performed strongly suggest that the simplifications and assumptions that are detailed above only weakly affect the final result. In particular, amplitude differences and non-stationary contributions to the Fourier transform have a much smaller effect on the mismatch than the intrinsic difference of various models, which we are interested in measuring here.

The interpretation of (7) is straightforward: the mismatch of hybrids is determined by the uncertainty of PN [restricted to the frequency range (f_1, f_m)] multiplied by the fraction of power that is coming from the PN part of the wave signal. This fundamental error, independent of the actual PN/NR fitting, is directly inherited from the differences of standard PN approximants and any PN/NR matching cannot be better than the result of (7). Therefore, one might think that analyzing the overlaps or fitting factors (or whatever strategy is appropriate) of different post-Newtonian approximants directly leads to conclusions of how reliable the hybrid is for a particular choice of f_m . When we compare, however, the mismatch of actual hybrid waveforms with the estimate (7) we find that the latter is considerably less than \mathcal{M} . In Fig. 1 we illustrate this fact for hybrids consisting of either the TaylorT1 or TaylorT4 approximant (in the form detailed in [41]; see also Sec. IV B) and the numerical data from the `SPEC` equal-mass run [52, 53]. The matching frequencies are chosen as

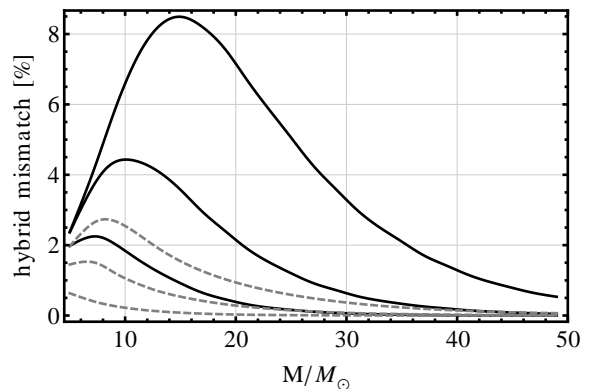


FIG. 1. Mismatch of nonspinning, equal-mass hybrid waveforms produced with either the TaylorT4 or TaylorT1 approximant. The lower bound (7), indicated as gray dashed lines, is compared to the actual mismatch of complete hybrid waveforms where the PN approximants are aligned to late merger NR data. The matching frequencies in each case are $M\omega_m \in \{0.04, 0.06, 0.08\}$ (from bottom to top).

$M\omega_m = 2\pi M f_m \in \{0.04, 0.06, 0.08\}$, and the stitching procedure is carried out in the Fourier domain as explained in [41].

Why is the mismatch that much greater than what is expected from PN in the given frequency range? The reason can be identified from the derivation of (7), where we effectively allow an optimal alignment (for each M) of both PN models while *independently* keeping the NR part *perfectly aligned*. In a true hybrid mismatch calculation, on the other hand, a time and/or phase shift always affects the *entire PN+NR hybrid*, and an optimal alignment of one part leads to a dephasing of the other. This effect is not caused by an erroneous matching, but an illustration of the fact that the optimal choice of t_0 and ϕ_0 in the sense of Eq. (4) is mass (frequency)-dependent for the PN models we consider.

Finally, by considering the obvious generalization of (7),

$$\mathcal{M} \geq \frac{\|h\|_{(f_1, f_m)}^2}{\|h\|^2} \mathcal{M}_{\text{PN}} + \frac{\|h\|_{(f_m, f_2)}^2}{\|h\|^2} \mathcal{M}_{\text{NR}}, \quad (8)$$

we can identify the three main contributions to the hybrid uncertainty: The PN and NR error, each weighted by the power they contribute to the signal and the misalignment caused by the fact that in the hybridization procedure the PN wave is aligned at high frequency which is potentially different from the optimal alignment for lower frequencies.

IV. HYBRID MISMATCHES

A. General procedure

The appealing prospects of (7) have been that the waveform error could be estimated only by the construction of the different PN approximants and the knowledge of the power contained in both the PN and NR part of the signal. In particular, a detailed understanding of the phase evolution beyond f_m was

not required. Fig. 1, however, made clear that the simple form of (7) is not sufficient to accurately estimate \mathcal{M} because the dephasing of the NR part is neglected.

We shall illustrate in this section that there is indeed a slightly generalized algorithm that *accurately* predicts the hybrid mismatch only with the ingredients listed above. A similar approach was recently suggested by Boyle [44] who realized that it is sufficient to combine PN approximants with *ersatz* NR data which he takes from the EOBNR model [15, 16, 30, 34]. We independently derive an algorithm here that is based on the same perceptions but highlights that no NR phase information *at all* is needed.

Let us consider a BBH system with fixed physical parameters. As before, our error measurement assumes the construction of two hybrid waveforms that differ in the PN part only. Their overlap reads

$$\begin{aligned} \mathcal{O}(h_1, h_2) &= \max_{\phi_0, t_0} \left[4 \operatorname{Re} \int_{f_1}^{f_2} \frac{\tilde{h}_1(f) \tilde{h}_2^*(f)}{S_n(f)} \frac{df}{\|h_1\| \|h_2\|} \right] \quad (9) \\ &= \max_{\phi_0, t_0} \left[4 \operatorname{Re} \int_{f_1}^{f_2} \frac{|A_1 A_2|}{S_n} e^{i(\phi_1 - \phi_2)} e^{i(2\pi f t_0 + \phi_0)} \frac{df}{\|h_1\| \|h_2\|} \right], \end{aligned}$$

where $A_i = |\tilde{h}_i|$ and $\phi_i = \arg \tilde{h}_i$. The effect of a time and phase shift of one waveform with respect to the other is explicitly written out in the second exponential term.

Assuming two PN models (PN1 and PN2) combined with the same NR waveform we trivially have

$$\phi_1 - \phi_2 = \begin{cases} \phi_{\text{PN1}} - \phi_{\text{PN2}} & , f < f_m \\ 0 & , f \geq f_m \end{cases} \quad (10)$$

The open question is the functional form of the PN phase-difference (or simply the PN phase error) in the case where the NR part of h_1 and h_2 are perfectly aligned. Here we have to apply an actual matching procedure, although we can use any preferred method *without* having NR data at hand. The key property of (10) we are exploiting is that only PN-PN differences are taken into account, and a direct PN-NR comparison is not necessary. The only input we need from NR simulations is the amplitude $|\tilde{h}| = A_1 = A_2$ for $f > f_m$. A good estimate for that can be taken from phenomenological models, such as [40] or [41], where the Fourier-domain amplitude is approximated by a closed-form analytic description.

The final global time and phase shift used in (9) to maximize the overlap is simply a (phase shifted) inverse Fourier transform of the remaining integrand. Its maximal real part is obtained by choosing ϕ_0 (for any t_0) such that the generally complex number lies on the real axis.

Based on that, our final algorithm for estimating hybrid mismatch errors caused by the uncertainty in the PN model is the following

1. Calculate the two different PN waveforms expressing the uncertainty to be quantified.
2. Apply the matching procedure such that one PN approximant is matched to the other at f_m (as if it were the NR waveform).

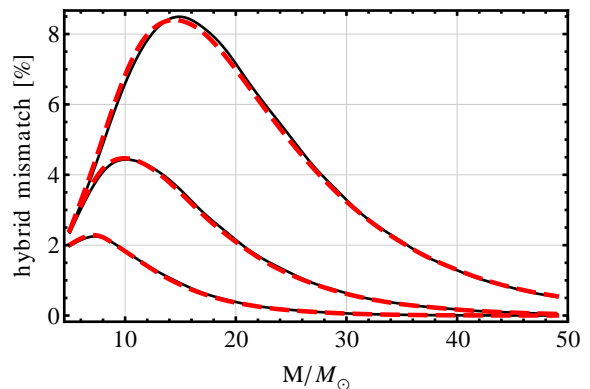


FIG. 2. Hybrid mismatches in the equal-mass, nonspinning case. Black solid lines are mismatches of actual TaylorT1/T4+NR hybrids, whereas the dashed (red online) lines are our estimates obtained without directly using any NR data (NR amplitude taken from a phenomenological model). The matching frequencies are from bottom to top $M\omega_m = 0.04, 0.06, 0.08$.

3. Fourier transform the so-aligned PN waveforms and keep the data for $f \in [f_1, f_m]$.
4. Complete the waveforms in the Fourier-domain by using an existing expression for the amplitude in the range $f \geq f_m$, e.g. from [40, 41] or from a short NR simulation. Set the phase in this regime to 0 (or any other function, but equal for both \tilde{h}_1 and \tilde{h}_2).
5. Calculate the overlap of \tilde{h}_1 and \tilde{h}_2 by maximizing the magnitude of the inverse Fourier transformation.

As expected by the relatively small effect of the amplitude on the mismatch calculation, this method is fairly robust with respect to the chosen amplitude description in the NR regime. In fact, the dashed lines in Fig. 2 use the recipe detailed in [41] but there is no noticeable difference when we use the formulas presented in [40]. In all cases we find excellent agreement with the actual PN+NR hybrid mismatches, see Fig. 2.

B. Application

Now that we have established an algorithm to predict the full waveform mismatches, we can exploit the computationally cheap procedure and calculate \mathcal{M} for many different physical scenarios. Our aim is to show how “reliable” the final combination of PN and NR waveforms is in different points of the parameter space.

First, let us highlight again that ideally, we are interested in the mismatch of the approximate waveform model to the true one. Since we cannot calculate the latter (which would also make the whole discussion pointless), we estimate the PN uncertainty by calculating the mismatch between different approximants. This can certainly be no more than a rough estimate since we are not aware of any principle that would guide us to which approximants at which PN order should be compared in order to obtain a well-defined notion of the PN error.

To still reach some understanding of the uncertainty in currently used high-order PN models we present the anticipated hybrid mismatches when approximants commonly denoted by TaylorT1, TaylorT4 and TaylorF2 are used. TaylorT1 and T4 are solutions of ordinary differential equations in the time domain describing the adiabatic inspiral of the BBH on quasi-circular orbits, whereas TaylorF2 is a frequency-domain description based on the stationary phase approximation. Details on these approximants can be found, e.g., in [7, 8] and references therein. We mainly employ the equations presented in [41], but with an updated 2PN spin-spin contribution from [51], see [54] for a collection of explicit expressions. Throughout this paper, we always employ the highest currently determined PN order, i.e., 3.5PN accurate phasing with spin contributions up to 2.5PN (and incomplete terms at higher order) and the 3PN amplitude expansion [50] including up to 2PN spinning corrections [51].

As in the construction of phenomenological models, we restrict the parameter space to black holes with comparable masses and spins aligned or anti-aligned with the orbital angular momentum of the binary \mathbf{L} (with its unit vector denoted by $\hat{\mathbf{L}}$). Then, each spin can be parameterized by just one dimensionless quantity,

$$\chi_i = \frac{\mathbf{S}_i \cdot \hat{\mathbf{L}}}{m_i^2}, \quad i = 1, 2, \quad (11)$$

where m_i and \mathbf{S}_i are mass and spin of the individual black hole, respectively. By exploiting a degeneracy in the spins, as observed in [55, 56], the parameter space can be further reduced, and we only use the mass-weighted total spin

$$\chi = \chi_1 m_1/M + \chi_2 m_2/M \quad (12)$$

and the symmetric mass-ratio

$$\eta = \frac{m_1 m_2}{M^2} \quad (13)$$

to label the different physical setups. (In fact, in the following analyses, each point with fixed χ is represented by $\chi_1 = \chi_2 = \chi$.)

To assess how the accuracy of currently feasible hybrid waveforms varies in the parameter space, we apply the algorithm outlined in Sec. IV A for different mass-ratios ranging from equal masses to 4:1, with spin magnitudes from -0.9 to 0.9 in each case. For every pair (η, χ) one obtains mass-dependent mismatches in the form of Fig. 2 that generally increase with increasing matching frequency $M\omega_m$.

Several plots illustrating this behavior can already be found in the literature. Contour plots of the mismatch as a function of mass and matching frequency are the main result of [44], and we obtain similar results by continuously varying $M\omega_m$, e.g., in Fig. 2. Taking the maximum mismatch with respect to the total mass instead (i.e., only considering the peaks in Fig. 2) Fig. 4 in [45] shows the inaccuracy of TaylorF2 hybrids compared to EOBNR as a function of the matching frequency. Fig. 11 in [43] presents a similar study with Taylor approximants and actual NR data. Given some slightly different choices in our approaches (especially lower cutoff frequency

and detector noise curve) the results we obtain are fully consistent with the numbers presented in the articles mentioned.

Generally, the conclusions [43–45] draw are sobering regarding GW detections and parameter estimation. The mismatches found are too high, current numerical relativity waveforms are *by far* too short and hybrids are consequently too inaccurate. In the following, we illustrate the basis of these statements and expand the existing knowledge by exploring the parameter space. To reduce the dimensionality of the problem, we calculate the maximum of the mismatch with respect to the total mass and fix $M\omega_m = 0.06$ (which corresponds to 10 GW cycles before the maximum of $|h(t)|$ in the equal-mass case).

In Fig. 3 we show contour plots that compare either TaylorT1 with TaylorT4 hybrids or TaylorT1 with TaylorF2 hybrids. The matching frequency is fixed at $M\omega_m = 0.06$. Certainly, we could include many more variants of PN approximants (including different versions of EOBNR), but we find it sufficient to present some general conclusions that become already clear from the examples chosen here. As reported before [42, 45] we see that deviating from equal mass cases, the disagreement generally becomes larger. This effect is even more pronounced when increasing spin magnitudes are considered. Heuristically we can understand the worse performance for increasing spins by the simple fact that spin contributions are only determined up to 2.5PN order, whereas non-spinning terms are known up to relative 3.5PN order. Surprisingly, the ‘island’ or ‘band’ of minimal mismatch does not occur strictly around vanishing spin magnitudes, indicating that different approximants can *by chance* agree extremely well in some portions of the parameter space. For completeness, let us report that the TaylorT4/TaylorF2 mismatch yields a pattern similar to the right panel of Fig. 3 but with minimal values moved to weakly positive spins.

The conclusions suggested by Fig. 3 and results from previous work [41, 43, 44] are indeed disappointing. If the mismatches caused by different PN approximants is actually a reasonable estimate for the uncertainty in currently practical hybrid waveforms, then values up to $\mathcal{M} \approx 50\%$ are certainly unacceptable. Reducing the matching frequency, thereby demanding longer NR waveforms, does reduce the mismatch everywhere, but it leads to unrealistic requirements in many portions of the parameter space.

To illustrate this, Table I addresses two important questions that form the basis of our TaylorT1/TaylorF2 comparison, listing selected points in the parameter space. First, what is the required matching frequency if a desired accuracy has to be fulfilled? Note that due to our algorithm we overcome the restriction of currently available NR waveform lengths that the authors in [41, 43] were facing. We also do not rely on assuming a particularly promising ‘candidate waveform’ to act as a long NR waveform as was done in [42, 44]. In fact, phase information above $M\omega_m$ are not required and do not enter the result; we can simply apply our algorithm to arbitrarily small matching frequencies. For each set of parameters we maximize the mismatch with respect to the total mass M (which we, however, restrict to $M \geq 5M_\odot$ for computational reasons) and thus obtain the monotonically increasing

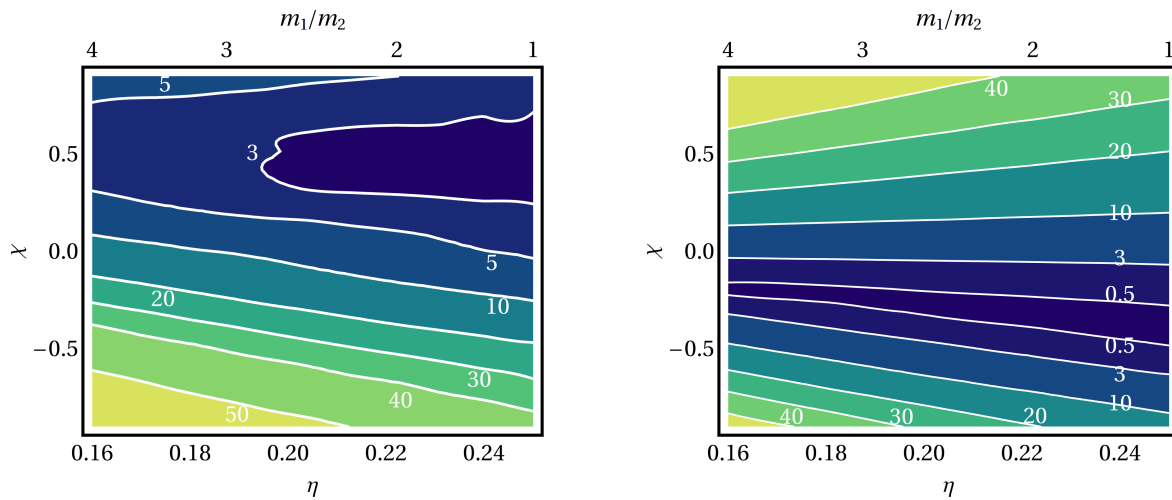


FIG. 3. Contour plots of the mismatch (in %) between different fictitious hybrids, as a function of the symmetric mass-ratio η and equal aligned spins with dimensionless magnitude χ . *Left panel:* PN part either defined by the TaylorT1 or TaylorT4 approximant. *Right panel:* Comparison of TaylorT1 and TaylorF2 in the PN part.

q	χ	$M\omega_m [\times 10^{-2}]$		$M_{\min}/M_{\odot} (M\omega_m = 0.06)$	
		$\mathcal{M} < 3\%$	$\rho_{\text{eff}} < 20$	$\mathcal{M} < 3\%$	$\rho_{\text{eff}} < 20$
1:1	0.0	3.93 (23)	1.15 (212)	15	40
1:2	0.2	2.40 (68)	0.99 (313)	25	49
1:3	0.5	1.70 (155)	0.84 (499)	33	57
1:4	0.8	1.38 (268)	0.75 (730)	38	61

TABLE I. Faithfulness of hybrid waveforms based on a TaylorT1/TaylorF2 comparison for selected physical parameters. The required matching frequency is reported if either a 3% maximal mismatch \mathcal{M} can be tolerated or if the error should be indistinguishable for SNRs less than 20, see (6). The parentheses indicate the number of GW cycles to the maximum of $|h(t)|$. The two right columns assume $M\omega_m = 0.06$ and give the minimal mass, where the waveforms are accurate enough in the sense described above.

function $\max_M \mathcal{M}(M\omega_m)$. By demanding either $\mathcal{M} < 3\%$ as the most relaxed requirement or the more stringent case of indistinguishable differences for effective SNRs of at most 20 [see (6)] we obtain the values given in Table I. In parentheses we also give the number of gravitational wave cycles from $d\phi_{\text{GW}}/dt = \omega_m$ to the maximum of $|h(t)|$ as predicted by the phenomenological waveform model [41].

It is unlikely that the typical length of “long” numerical waveforms will change by an order of magnitude before the advent of Advanced LIGO, and so a more practical question is: given a currently achievable NR waveform length, in which mass-range is the PN+NR hybrid accurate enough? As an example we assume again a matching frequency of $M\omega_m = 0.06$ and show on the right-hand side of Table I the minimal masses the hybrid is accurate for in the sense detailed above. For comparison, the pure NR part occupies the entire frequency band down to 20Hz for masses $M \geq 97M_{\odot}$. Note that, distinct from [45], we do not consider errors *above* $M\omega_m$ since we are

concerned with *hybrids* and not possibly fitted closed-form waveform models that introduce additional errors. Therefore, our values for M_{\min} are less than the corresponding results in [45] that are based on the comparison of EOBNR and the phenomenological model of [40].

The obvious message from Table I is that *in general* extremely long NR simulations would be needed to overcome the intrinsic uncertainty in standard PN formulations for given physical parameters. For NR waveforms containing so many cycles our assumption that their intrinsic error can be neglected is possibly no longer valid, which would lead to even higher modeling errors. Anyway, the numbers presented are only an ‘order of magnitude’ estimate in this most conservative approach. The reader should always keep in mind that our notion of error is based on comparing different, at highest available order, consistent PN descriptions and especially concrete statements for particular points in parameter space may be spoiled by an (un)fortunate choice of approximants (see a similar discussion in [42]). More importantly, as we shall show in the next section, fixing the physical parameters of the waveforms from the outset greatly overestimates the uncertainty for signal detection.

V. FITTING FACTORS

A. General

The accuracy assessment presented in Section IV only allows for very limited conclusions about the actual utility of hybrid waveforms in various applications. Apart from the restrictions coming from our limited understanding of the PN error there is also an important fact we have neglected so far: in astrophysically relevant applications the knowledge of physical parameters like total mass, mass-ratio and spin is never *exact*. If a set of hybrid waveforms constitutes a *waveform fam-*

ily which is used to extract information from an unknown signal, then the standard matched-filter procedures rely on varying (and maximizing with respect to) such parameters. The accuracy of the predicted ‘best-fit’ parameters is once again limited by the detector noise and the modeling error and even if the latter exceeds the first, one may still argue that a tolerated bias does not significantly reduce the scientific output from GW detections.

In this section we shall therefore consider combinations of NR data with a particular PN approximant as the ingredients of an entire manifold of waveforms, parameterized by an absolute time and phase scale (t_0 and ϕ_0) as well as the physical parameters introduced before: M (total mass), η [symmetric mass-ratio (13)] and χ [spin combination (12)]. The efficiency of detecting a signal defined by t_0, ϕ_0, M, η and χ is properly quantified through the fitting factor

$$\text{FF} = \max_{M', \eta', \chi'} \mathcal{O} \left[h_1(M', \eta', \chi'), h_2(M, \eta, \chi) \right]. \quad (14)$$

Note that the maximization with respect to t_0 and ϕ_0 is already included in the definition of the overlap \mathcal{O} , see (9).

The accuracy threshold for detection we quoted before is indeed defined including this additional maximization, i.e., in terms of

$$\mathcal{M}_{\text{FF}} = 1 - \text{FF}. \quad (15)$$

If a waveform family $\{h_1\}$ satisfies $\mathcal{M}_{\text{FF}}(h_1, h_2) < \mathcal{M}_{\text{max}}$ then it is said to be *effectual* in the detection of h_2 [5]. The results in Sec. IV are only a lower bound on this effectualness.

The accuracy requirements for parameter estimation are naturally more demanding than those for detection. In the recent literature [41, 43, 45, 46] the *faithfulness* of waveforms was usually defined by the criterion (5) (without optimization with respect to physical parameters), thereby demanding that the maximal information can be extracted from the data without being restricted by the model itself. Here, however, we want to understand faithfulness in the original sense introduced in [5] that is based on the difference of the target waveform parameter λ with the recovered model parameter $\tilde{\lambda}$ for which (14) is maximal. If this bias $\Delta\lambda = \tilde{\lambda} - \lambda$ is small enough, we can still accept the waveform model family as accurate enough, even for parameter estimation. Therefore, by analyzing \mathcal{M}_{FF} and the corresponding parameters we can sensibly make analogous conclusion as before, but based on the actual optimization strategy that is employed in current template-based GW searches.

Due to the additional freedom of varying physical parameters we now have to calculate the *ambiguity function*

$$\mathcal{A}(\lambda', \lambda) = \mathcal{O} \left[h_1(\lambda'), h_2(\lambda) \right] \quad (16)$$

between hybrids constructed from the same set of NR waveforms but members of different PN approximants. It depends on the parameters of the waveforms, λ' and λ , as well as the waveform models themselves.

Since the phase difference above $M\omega_m$ in the overlap integral (9) does not vanish generally for $\lambda' \neq \lambda$, we have to

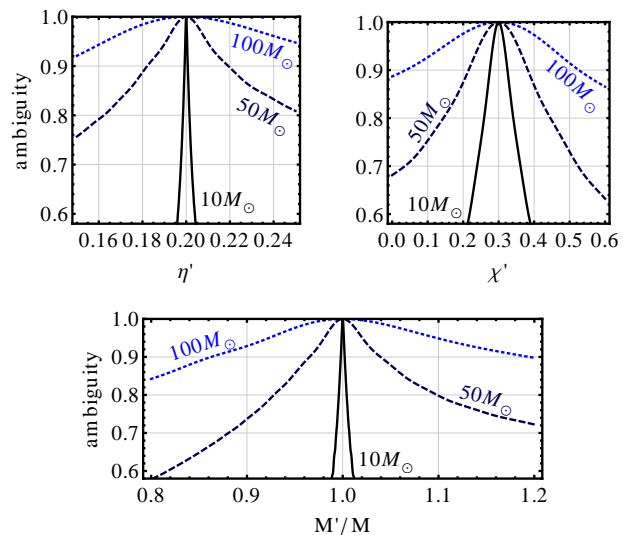


FIG. 4. The ambiguity function (16) between two phenomenological waveforms [41], where h_2 is fixed with $\eta = 0.2$, $\chi = 0.3$ and the total mass as indicated in the plots. The parameters of h_1 are varied individually while the others are kept constant at the values of h_2 , respectively.

slightly modify the algorithm presented in Sec. IV A. In particular, we now need an estimate of how small changes in physical parameters affect the phase difference in the assumed NR regime. (The PN regime is affected as well, but there is no qualitative difference to the PN comparison incorporated before.) One possible strategy to quantify phase changes along variable physical parameters is to perform a number of numerical simulations and interpolate between the data obtained. Depending on the density of samples in the η and χ directions (the scaling with M is given trivially by a single simulation), such a procedure can be very time- and resource-consuming. However, the phenomenological fittings performed in [38–41] have utilized exactly this type of interpolation, and we conveniently use the result of [41] here because the fitting there is localized to frequencies close to and in the NR regime.

Finally, to ensure the proper relative alignment, our algorithm to calculate \mathcal{A} for arbitrary (in practice small) variations in all parameters is to match different PN approximants to a phenomenological waveform (phase and amplitude) that is used above $M\omega_m$ resulting in a hybrid $\tilde{h}(f; M, \eta, \chi, t_0, \phi_0)$.

Let us highlight that although we are now building PN+phenomenological hybrids our analysis is not assessing how accurate individual waveforms describe the entire coalescence process. Note for instance that we could have introduced this hybridization concept already in the previous section, but, as we have shown, the phase above the matching frequency did not enter the overlap calculation. Similarly now, we use the phenomenological phase description merely to model the M -, η - and χ -dependence at higher frequencies. Fig. 4 illustrates what kind of information we are using by plotting slices of the ambiguity function of the phenomenological model with itself for the case $\eta = 0.2$ (mass-ratio ≈ 2.6), $\chi = 0.3$ and $M/M_\odot \in \{10, 50, 100\}$. In Sec. IV we

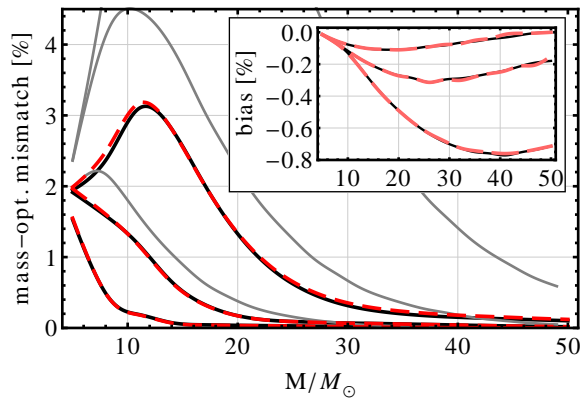


FIG. 5. The mass-optimized mismatch between equal-mass, non-spinning TaylorT1/TaylorT4+NR hybrids (black solid lines) compared to our NR-free estimate (dashed lines). The matching frequencies are $M\omega_m \in \{0.04, 0.06, 0.08\}$ from bottom to top. The gray lines show the results of non-optimized mismatches for comparison, see also Fig. 2. The inset illustrates the relative bias in the total mass (matching frequencies in reverse order).

only exploited $\mathcal{A} = 1$ for $\lambda' = \lambda$ whereas now we need an estimate of the shape of \mathcal{A} also for $\lambda' \neq \lambda$ (although for small $|\lambda' - \lambda|$).

We can make two immediate observations from Fig. 4. Especially for small masses we see that relatively small changes in, for instance, symmetric mass-ratio or total mass (the other parameters are kept constant, respectively) modify the waveform considerably, so that the high mismatches for equal parameters (reported, e.g., in Fig. 2) could potentially be reduced drastically by only small variations in the physical parameters of one model waveform. Although the formal criterion (5) for faithfulness (or better indistinguishability) failed, the fitting factor could still be extremely close to unity with a minimal bias in the parameters. The second interesting observation from Fig. 4 is that the width around the maximum of the ambiguity function increases towards higher masses so that a comparison of two waveforms is increasingly insensitive to parameter changes at higher frequencies. This in turn endorses our assumption that the fitting factors and biases we shall calculate are dominated by PN effects (and not the choice of data above $M\omega_m$) for small masses, where the accuracy requirements turned out to be hardest to satisfy.

B. Comparison with previous results

Before exploring fitting factors across the parameter space, let us present two examples that illustrate the general conclusions we shall draw in this paper. We first come back to the canonical equal-mass, nonspinning case and the TaylorT1/TaylorT4 comparison that was employed before (see Fig. 2 and [42]). To test the validity of our approach we again compare our estimate to hybrids constructed with actual NR data (matched at $M\omega_m \in \{0.04, 0.06, 0.08\}$, respectively). Due to the unavailability of NR data with arbitrary η and χ , we for now only maximize with respect to the total

mass M . Note that the results shown in Fig. 5 fully agree with the analysis of [42] (see Fig. 6 therein). They not only confirm that our combination of PN and phenomenological data accurately predicts the disagreement of the ‘true’ PN+NR hybrids, one can also observe the striking improvement when the additional maximization with respect to M is taken into account. The peak-mismatch without optimization was approximately 8.8%, 4.5% or 2.2%, depending on $M\omega_m$. With mass-optimization we instead find $\mathcal{M}_{\text{FF}} < 3.2\%$, 2.0% and 1.5%, respectively. The relative bias in the total mass, $(\bar{M} - M)/M$, is always less than 0.8% and the earlier the matching is performed the smaller the bias becomes.

A subsequent question that has not been answered so far is to what extent further optimizations, say along the symmetric mass-ratio and the spin(s) of the model system, improve the agreement between the waveform families even more. Reference [42] applied a crude estimation of the effect an additional mass-ratio optimization has, and concluded that a (total) mass-optimization alone serves as a sufficient assessment of the full fitting factor. We now find that this conclusion was incorrect. We illustrate the effect of further optimizations through the comparison of TaylorT1- and TaylorF2-based waveforms (matched at $M\omega_m = 0.06$) in Fig. 6. The TaylorT1 target signal is fixed as a system with mass-ratio 4:1 and spin $\chi = 0.5$, a point in parameter space that clearly fails all accuracy requirements when looking at Fig. 3. By maximizing with respect to M , however, the maximal mismatch drops from 32.2% to 10.4%. Varying all three considered physical parameters finally yields a curve with $\mathcal{M}_{\text{FF}} \approx 1.6\%$ at maximum, making the TaylorF2-based family accurate enough for detection. The relative bias in the parameters are less than 1% for M , of the order of 1% for η and $\lesssim 10\%$ for χ .

Note that a faithfulness analysis, as in Sec. IV and [43, 44], would conclude that NR waveforms with many hundreds of cycles are necessary to produce hybrids (and consequently waveform models) that are sufficient for parameter estimation purposes. Here we see that waveforms that we might at first sight regard as far too inaccurate, in fact may yield relatively small parameter biases when embedded in a waveform family.

The optimization algorithm with respect to physical parameters is computationally more challenging than maximizing the inner product with respect to t_0 and ϕ_0 only. For each set of test parameters (η, χ) we have to construct a new waveform. Since TaylorF2 is an analytical closed-form PN description that is fast to evaluate and our matching to the phenomenological model is performed directly in Fourier space [41] we only consider TaylorF2-hybrids as test waveforms h_1 . For the fixed target waveforms h_2 we chose to employ the TaylorT1 approximant, because it was shown in [57] that its (dis)agreement to pre-merger NR data is most robust over the considered parameter space and [44] noted that a maximal uncertainty estimate involves comparing to TaylorT1-inspirals.

Starting with equal parameters $\lambda' = \lambda$, we search for the nearest local maximum of the overlap $\mathcal{O}(h_1, h_2)$ by varying λ' along the gradient of the overlap. Thus, we ensure a quickly converging improvement after a relatively small number of iterations. The results we present, however, do not take into account the entire distribution of the ambiguity function and

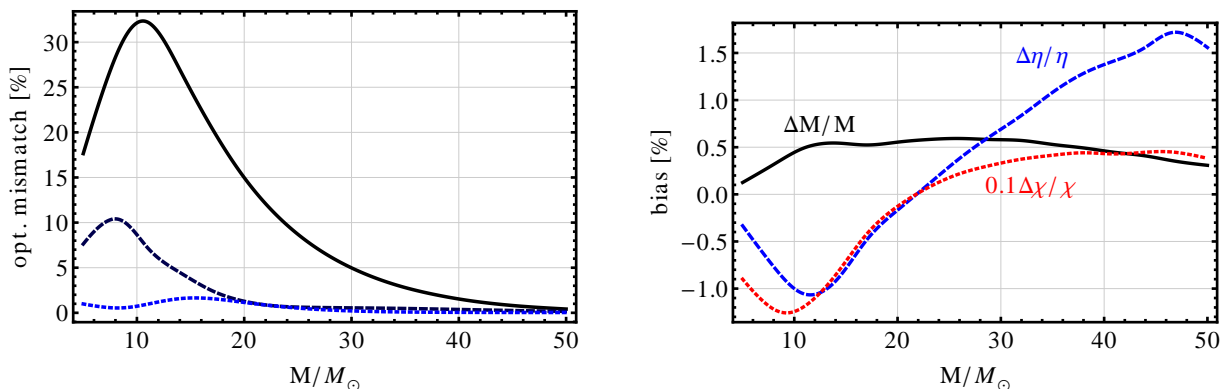


FIG. 6. Mismatch between TaylorT1- and TaylorF2-based waveforms for mass-ratio 4:1, $\chi = 0.5$ and matching frequency $M\omega_m = 0.06$ (left panel). The mismatch is not optimized (top solid line), mass-optimized (dashed line) or optimized with respect to all physical parameters of the TaylorF2-based model (lowest dotted line). The bias in the parameters are provided on the right panel.

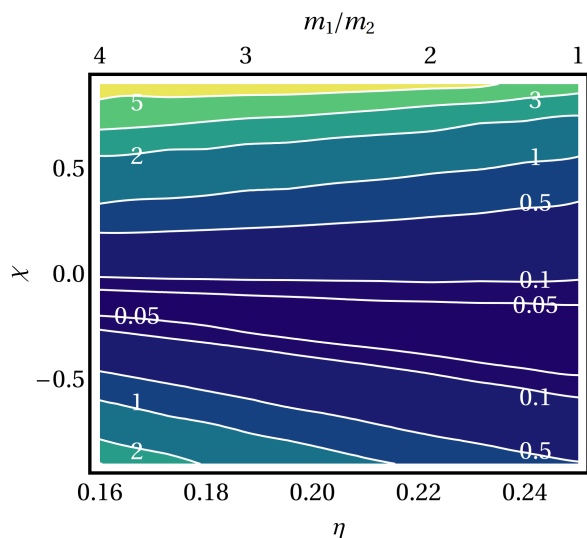


FIG. 7. The maximum of the optimized mismatch (in %) for hybrids constructed either with TaylorT1 (target signal) or TaylorF2 (template signal) and a matching frequency of $M\omega_m = 0.06$.

are still only a lower bound on the fitting factor. Given the tremendous decrease in mismatch for relatively small changes in physical parameters we argue nevertheless that this local extremum should serve as a reasonable estimate of the error one has to assume in terms of the fitting factor.

We repeated the exploration of the parameter space with a study similar to the one presented in Fig. 3. The matching frequency is again fixed at $M\omega = 0.06$ and we calculate \mathcal{M}_{FF} , Eq. (15), for masses $5M_\odot \leq M \leq 20M_\odot$. We checked that the mismatch decreases towards the boundaries of this interval, so that the enclosed maximum can indeed be regarded as the global extremum. After performing this maximization of the mismatch with respect to M for fixed (η, χ) , we present our results as a contour plot in Fig. 7. The structure is very similar to the pattern of the non-optimized mismatch, cf. the right panel of Fig. 3. The obvious difference is, however, that calculating the detection-relevant quantity \mathcal{M}_{FF} instead of the

diagonal mismatch $1 - \mathcal{A}(\boldsymbol{\lambda}, \boldsymbol{\lambda})$ results in numbers that are ~ 10 times less than what was considered before as error estimates.

This allows for very different conclusions: Even a moderate matching frequency like the one considered here leads to hybrids that are accurate enough for detection in a large portion of the parameter space. Simulating NR waveforms with few (< 10) orbits should hence be good enough for many applications considering systems with moderate spins and mass-ratios. Although this is a very broad statement, it is clearly distinct from previous analyses [43–45] that concluded *much longer* NR waveforms are needed to sensibly connect them to standard PN approximants.

Of course, Fig. 7 only shows the optimal agreement between the two considered waveform families and one might fear that the difference between simulated and recovered parameters is large in some parts of the parameter space. However, as anticipated by Fig. 6, the bias in total mass and symmetric mass-ratio are small, approximately $\pm 1\%$ and $\pm 1.5\%$ at most, respectively. The spin parameter χ is uncertain by $-0.15 \leq \Delta\chi \leq 0.05$. A deeper analysis of these biases is beyond the scope of this paper and results are likely more model-dependent than the general conclusions we present here.

For completeness, we note that for increasing values of the simulated spin, $\Delta\eta$ and $\Delta\chi$ generally decrease from positive to negative values, ΔM increases at the same time. This correlation is expected from the form of the PN expansion, where modifications of M can be compensated at lowest order by changing η inversely. Studies of PN approximants in [8] show similar tendencies, although the biases reported there are considerably higher due to the absence of a common NR part at high frequencies. The modeling biases we find should be compared to statistical errors of full waveform families. In the case of the nonspinning phenomenological model [39] a Fisher matrix study as well as Monte-Carlo simulations were presented in [58], and the uncertainties found for Advanced LIGO and signals of SNR 10 are $\Delta M/M \lesssim 3\%$ and $\Delta\eta/\eta \lesssim 8\%$ ($M < 100M_\odot$). These values are of the same order of magnitude than our results, and we take this as an indication that modeling errors do not vastly dominate the param-

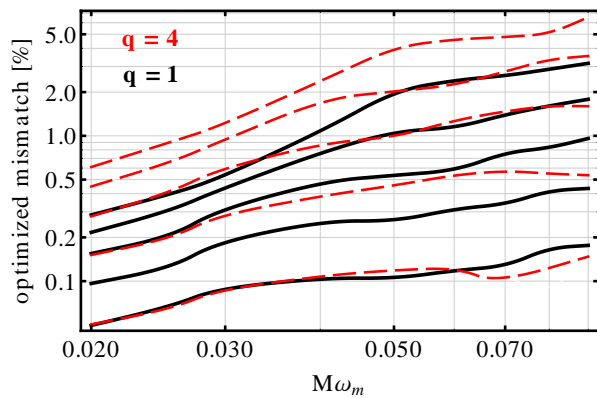


FIG. 8. The fully optimized mismatch \mathcal{M}_{FF} as a function of the matching frequency $M\omega_m$ for equal-mass systems (solid lines) and mass-ratio 4:1 (dashed lines). The considered spins in each case are $\chi \in \{0, 0.2, 0.4, 0.6, 0.8\}$ from bottom to top.

eter estimation uncertainty. However, further studies are underway [59] to determine statistical errors for spinning waveform models.

C. Model accuracy for spinning systems

These new results constitute much brighter prospects for currently feasible NR simulations than the conclusions drawn in Sec. IV and [42–45]. In certain parts of the parameter space, however, the mismatch error presented in Fig. 7 is still too high, particularly if one keeps in mind that gaining sensitivity of GW detectors is extremely difficult on the hardware side and theoretical considerations should reduce this sensitivity as little as possible [45]. Therefore, $\mathcal{M}_{\text{FF}} > 3\%$ for highly spinning systems should be improved by considering lower matching frequencies. Equally important is the question of whether numerical simulations for systems with moderate spins and mass-ratios can be considerably shorter than $M\omega_m = 0.06$ which we assumed so far.

In Fig. 8 we analyze the dependence of the mismatch error by showing the maximum of \mathcal{M}_{FF} as a function of $M\omega_m$. We consider equal masses and mass-ratio 4:1 with spins $\chi \in \{0, 0.2, 0.4, 0.6, 0.8\}$ in each case. Note that we do not include negative values of χ here, because the fact that the mismatch error for $\chi < 0$ is smaller and not monotonic in χ (see Fig. 7) is likely an artifact of our choice of PN approximants (recall the obvious differences in Fig. 3). As expected, Fig. 8 illustrates that reducing the matching frequency, e.g., from $M\omega_m = 0.08$ to $M\omega_m = 0.02$, leads to an improvement in mismatch by a factor of 2 to 10, depending on the spin.

Larger values of the spin generally yield larger mismatches which in turn leads to stronger requirements for $M\omega_m$, assuming a given accuracy goal. This is unfortunate because the orbital hangup configuration of positive aligned spins decelerates the frequency evolution in the inspiral of the binary, demanding even longer simulations for a given frequency range.

As such extremely long NR waveforms may not be available in the near future (including the Advanced LIGO era),

orbits	equal-mass	mass-ratio 4:1
5	1.5%: $-0.76 < \chi < 0.60$	3.0%: $-0.95 < \chi < 0.55$
	0.5%: $-0.37 < \chi < 0.31$	1.5%: $-0.52 < \chi < 0.39$
10	1.5%: $-1.00 \leq \chi < 0.70$	3.0%: $-1.00 \leq \chi < 0.68$
	0.5%: $-0.45 < \chi < 0.39$	1.5%: $-0.56 < \chi < 0.48$
20	0.5%: $-0.97 < \chi < 0.57$	3.0%: $-1.00 \leq \chi < 0.79$
	0.2%: $-0.28 < \chi < 0.22$	1.5%: $-0.92 < \chi < 0.55$

TABLE II. Range in spin parameter χ where a given accuracy requirement ($\mathcal{M}_{\text{FF}} < 3\%, 1.5\%, 0.5\%$ or 0.2%) is fulfilled. Each row specifies the assumed number of orbits before merger for the NR waveform (= number of GW cycles divided by 2).

we continue with a slightly different application of our results: How reliable is a set of complete waveforms constructed with standard PN approximants and NR simulations covering 5 (10, 20) orbits before merger (i.e., 10, 20 or 40 GW cycles prior to the maximum of $|h(t)|$)? To quantify these uncertainties we have to combine an estimate of the minimal matching frequency allowed by such NR waveforms with the resulting mismatch error from Fig. 8. We calculate the first from the inverse Fourier transform of the phenomenological model [41] and the time-derivative of the phase, $M\omega_m \approx d \arg h(t_n)/dt$, where $\arg(t_n) = \arg h(t_{\text{max}}) - n2\pi$ ($n = 10, 20, 40$, respectively), and t_{max} is the time of the maximum amplitude $|h|$. This spin- and η -dependent value is then taken into the results presented with Fig. 8 to estimate \mathcal{M}_{FF} for each configuration. Note that we use a more pessimistic error estimate for anti-aligned spins ($\chi < 0$) by assuming the mismatches of $|\chi|$ due to the reasons discussed above.

One kind of possible conclusion one can then draw is summarized in Table II for equal masses and mass-ratio 4:1. Given an accuracy goal (which we take as either 3%, 1.5%, 0.5% or 0.2%) we provide the range of spins in which hybrids with the specified number of NR orbits fulfill this goal. Note that the asymmetry in the spin parameter is only caused by the different matching frequencies waveforms with constant length permit. Again, we can very clearly see that even relatively short waveform are good enough for detection. In fact, mismatches of 0.5% are below the noise level for SNR 10, and differences of 0.2% are indistinguishable for SNR $\lesssim 16$ according to Eq. (6). However, one can also see from Table II that doubling the number of orbits does not enlarge the accuracy range dramatically in many cases, although such simulations would take far more computer power and time.

D. Nonspinning unequal-mass systems

So far, we refrained from explicitly calculating mismatches for mass-ratios $> 4:1$ here because our underlying phenomenological model was only calibrated to numerical simulations with mass-ratios $\leq 4:1$. Pushing the model beyond these values would add another uncertainty in addition to the way we estimate PN errors already, and more elaborate studies

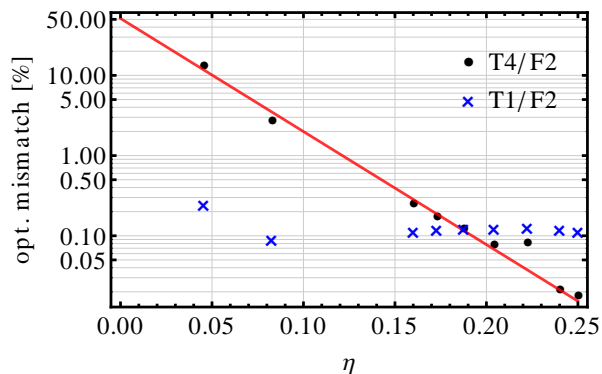


FIG. 9. The fully optimized mismatch of nonspinning target signals employing either the TaylorT1 or TaylorT4 approximant with model waveforms constructed with TaylorF2 inspirals. The assumed matching frequency is always $M\omega_m = 0.06$. The bias in parameters is $|\Delta M|/\bar{M} \lesssim 0.6\%$ (0.16%), $|\Delta\eta|/\bar{\eta} \lesssim 1.0\%$ (0.3%), $|\Delta\chi| < 0.04$ (0.017), where the values in brackets indicate the restriction to $q \leq 4$.

(possible including different models such as [40] and variants of EOBNR) are needed to reach sound conclusions.

Nevertheless, numerical simulations of higher mass-ratios are potentially interesting, and we shall try to estimate their reliability on the basis of our (extrapolated) knowledge here. We restrict this study, however, to nonspinning target signals. These are the systems where we do not expect the PN errors to drop significantly on the timescale of Advanced LIGO (in contrast to spinning binaries, where higher order PN terms may well be calculated in the next few years). We find that the agreement between TaylorT1- and TaylorF2-based hybrids is exceptionally good along $\chi = 0$ (see Figs. 7 and 9). In contrast, the TaylorT4/TaylorF2 uncertainty increases towards higher mass-ratios (smaller values of η) as we would expect from the form of the PN expansion. Therefore, we shall conservatively base our statements on comparing TaylorT4 and F2 approximants in this section.

To illustrate our argument, we plot in Fig. 9 the maximum of the fully optimized (i.e., with respect to M , η and χ) mismatches between TaylorF2 and either TaylorT1 or TaylorT4 hybrids, all matched to fictitious NR data at $M\omega_m = 0.06$. The fixed target parameters are chosen as $\chi = 0$ with the mass-ratio q varying from 1 to 4 in steps of 0.5 as well as $q = 10$ and $q = 20$. While the comparison with TaylorT1 yields weakly η -dependent mismatches below 0.3%, TaylorT4 target signals exhibit a steeply increasing divergence from the model signals towards higher mass-ratios. Its approximately exponential behavior is well described by the following fitting formula

$$\log_{10} \mathcal{M}_{\text{FF}} \approx -0.29 - 14.1\eta \quad (17)$$

which is included as a straight line in Fig. 9. A conservative estimate of the general model uncertainty would be the maximum of both data series for each η , i.e., (17) for small η and roughly constant $\mathcal{M}_{\text{FF}} \approx 0.12\%$ for $\eta > 0.1866$ ($q < 3$).

Evidently, a matching frequency of $M\omega_m = 0.06$ is only good enough for $\eta > 0.081$ ($q < 10.2$) if a mismatch of at most 3% is tolerated. Again, reducing the matching frequency helps to increase the accuracy of the final waveform, and we

orbits	mass-ratio	$q = 20$
5	3.0%: $q < 8.9$	$\max_M \mathcal{M}_{\text{FF}} \approx 15\%$ ($19M_\odot$)
	1.5%: $q < 6.8$	$21M_\odot$: 12%, $63M_\odot$: 0.3%
10	3.0%: $q < 11.4$	$\max_M \mathcal{M}_{\text{FF}} \approx 8.2\%$ ($13M_\odot$)
	1.5%: $q < 8.6$	$21M_\odot$: 3.0%, $63M_\odot$: 1.6×10^{-5}
20	3.0%: $q < 14.8$	$\max_M \mathcal{M}_{\text{FF}} \approx 5.7\%$ ($11M_\odot$)
	1.5%: $q < 10.7$	$21M_\odot$: 0.8%, $63M_\odot$: 6.4×10^{-6}

TABLE III. Accuracy of nonspinning hybrid waveforms, based on combining PN TaylorT4 or TaylorF2 data with NR waveforms of specified length (defined by the number of orbits before merge = number of GW cycles divided by 2). *Left column*: Range in mass-ratio where a given accuracy requirement ($\max_M \mathcal{M}_{\text{FF}} < 3\%$ or 1.5%) is fulfilled. *Right column*: Mismatch error for $q = 20$, both at maximum of all masses (location indicated in parentheses) and at astrophysically motivated minimal values of the total mass (see text).

systematically analyze how useful numerical simulations of 5, 10 or 20 orbits before merger are in the nonspinning unequal-mass regime. For that, we calculate $\max_M \mathcal{M}_{\text{FF}}$ as a function of the matching frequency and the symmetric mass-ratio, similar to what was done for Fig. 8. The matching frequency is then converted to orbits before merger as explained in the previous section.

In Table III we present our results in analogy to Table II, where we provided the range of the spin parameter χ in which the waveform model meets certain accuracy requirements. Now we complement the picture by restricting ourselves to the nonspinning case; our error estimates are based on optimized TaylorT4/TaylorF2 hybrid mismatches, and we present the accuracy range in terms of the mass-ratio. Note that, although only five orbits of NR data before merger are sufficient for detection for most of today's standard simulations ($q \lesssim 6$), even the computationally very challenging goal of 20 orbits before merger is not enough to reliably model mass-ratios as high as 15 or more for arbitrary total masses of the binary.

It should be pointed out, however, that we report the worst disagreement between the considered hybrids in the left column of Table III, i.e., we demand that the assumed accuracy requirement is satisfied for *all* values of the total mass. As discussed in [44] already, one should rather understand the mismatch error and the accuracy requirement as functions of the total mass. After all, binaries with larger total mass have higher SNR in the detector (for constant distance of the source). More important for us here is that some of the considered astrophysical scenarios may not even exist or be extremely unlikely, and if the modeling error exceeds accuracy thresholds in these regions, we do not have to bother.

We illustrate this argument with a concrete example: The (fictitious) waveform of a binary with mass-ratio 20:1 exhibits the largest uncertainty at total masses less than $20M_\odot$, depending on the matching frequency (the values for NR simulations covering 5, 10 or 20 orbits before merger are given in parenthesis in the right column of Table III). If we only consider *black holes* as objects in the binary and follow observational [60] and theoretical [61] evidence that their individual masses

are $> 3M_{\odot}$, then the lowest total mass to consider in our error analysis is instead $63M_{\odot}$. With our idealized assumptions, this is a regime where the mismatch drops monotonically with increasing total mass (due to the dominating amount of exact high frequency data), and the maximal uncertainty at $63M_{\odot}$ proves to be more than sufficient for detection purposes, even with only a few NR orbits; see Table III. In this sense, modeling higher mass-ratios is more accurate than comparable masses, as [44] noted already for diagonal (non-optimized) mismatches.

One the other hand, one could argue that the smaller object in the 20:1-binary could also be a neutron star. If the companion is a much heavier black hole, tidal effects are extremely weak [27] and the plunge is hardly affected from finite size effects of the neutron star [62]. Thus, we may hope to accurately capture these systems with a BBH template family as well, and smaller total masses have to be considered. According to [63], (proto)neutron stars are expected to have masses $> 1M_{\odot}$, which is in agreement with current observations (see [64] for an overview). Assuming the lower bound of $1M_{\odot}$ for the mass of a single compact object, we consequently have to consider total masses down to $21M_{\odot}$ (for $q = 20$) which leads to higher modeling uncertainties in the waveform. However, as Table III shows, 10 NR orbits before merger would be virtually good enough for detection purposes, 20 orbits already yield a mismatch of only 0.8% at $21M_{\odot}$. Hence, even the theoretically and numerically difficult unequal-mass regime may well be modeled with only a few NR orbits, given the astrophysical expected properties of such systems.

Of course, these astrophysical limitations are highly uncertain, and the conservative error analyses are the ones presented in Table II and the left column of Table III. However, given that caveat, we conclude that currently feasible numerical simulations are potentially good enough to model in combination with PN approximants an important fraction of the parameter space.

VI. DISCUSSION

Predicting the GW signature of an inspiraling and merging BBH in General Relativity is inevitably associated with analytical or numerical approximations to the full theory, which introduce errors in the final result $h(t)$ or $\tilde{h}(f)$. In this paper we estimated these errors by the distance between two approximate solutions for each physical configuration. While neglecting uncertainties on the NR side, we assumed different standard PN approximants in a frequency range up to the point where the waveform is matched to an NR-based merger and ringdown model.

We quantified the uncertainties by comparing the currently available 3.5PN (spinning contributions up to 2.5PN) versions of TaylorT1, TaylorT4 and TaylorF2 approximants. Introducing a simple algorithm that only requires amplitude information beyond the matching frequency, we first confirmed previous studies [42–44] that found that the mismatch error for fixed physical parameters greatly exceeds reasonable accuracy requirements, assuming typical NR waveform lengths.

Instead of demanding extremely long numerical simulations to overcome this uncertainty in the modeling process, we refined the understanding of the waveform error by adopting the actual data analysis strategy of detecting an unknown signal in noise-dominated interferometer data. In particular, assuming waveform families instead of individual waveforms naturally redefines the concept of distance by allowing physical parameters to be varied in the mismatch calculation.

The results presented in Sec. V indicate then that the GW signatures for many astrophysically relevant systems can in fact be well modeled by straightforward combinations of standard PN approximants and currently feasible NR simulations, covering < 10 orbits before merger. Although the accuracy has not yet reached a level such that detection and parameter estimation errors are limited only by the detector noise for high SNR events, the reported disagreement among different models and biases in the parameters are certainly tolerable for the first GW detections that are likely to have low SNRs (~ 10). While this is true for systems with moderate spins, one has to keep in mind that even our idealized setting yields mismatch errors for high values of spins that are of the order of a few percent, which increase for higher mass ratios. Reducing the matching frequency poses unrealistic challenges for current NR codes, and either fundamentally different numerical approaches or advances in PN are needed to fully control the entire parameter space.

While the next spin-contributions in PN theory may become available in the near future to further improve the modeling of spinning systems (see the recent calculations of next-to-next-to-leading order spin-orbit contributions [65, 66]), unequal-mass nonspinning contributions at 4PN order are unlikely to be calculated with established techniques soon. However, as we discussed for a binary with mass-ratio 20:1, astrophysical expectations are that such systems only form with a high total mass, thereby reducing the impact of PN uncertainties. Even for 20:1 binaries, our results suggest that NR simulations of less than 10 orbits are sufficient.

In summary, we found that not single hybrid waveforms, but rather the embedding in the waveform manifold, results in templates accurate enough for detection, even with today's limited number of NR orbits. The uncertainty in physical parameters we had to accept for this tremendous increase in overlap is rather small, $\sim 1\%$ in mass and symmetric mass-ratio, and ~ 0.1 at most for the spin parameter χ . For nearly equal-mass systems, the individual masses of the constituents are then only reliable to

$$\frac{\Delta m_i}{m_i} \approx \frac{\Delta M}{M} + \sqrt{\frac{\Delta \eta}{\eta}} \sim 10\%, \quad (18)$$

and it has to be decided whether this is good enough for astrophysical studies.

Of course, our analyses are meant to provide a general concept of how to deal with modeling errors, instead of giving final answers. Especially, as we emphasized throughout the paper, we do not address the question of how accurate a particular waveform model is. The statements formulated here are based on selecting PN approximants that are compared with

each other, and our choices were made to result in conservative estimates illustrating the *order of magnitude* one generally has to assume for our notion of error. One should nevertheless keep in mind that a particular PN+NR combination can be much closer to the real waveform than estimated here, as well as the possibility that the PN ambiguity at consistent 3.5PN order generally underestimates the true error in the signal description.

It should be noted further that the numbers we find rely on two essential assumptions: We neglect both the error of the hybridization procedure and any uncertainties beyond the matching frequency. Both assumptions are well motivated by previous studies [21, 41–43], but care has to be taken when generalizing their validity. For instance, from Fig. 7 or Table II one might be tempted to conclude that actually very short NR waveforms are enough for modeling equal-mass, hardly spinning systems. This is certainly true from our results if the matching to PN can be done unambiguously. However, if there are too few cycles to align PN and NR signals properly, different matching procedures may lead to very different results. This aspect was not treated here as it can be checked separately, and it should only affect the resulting waveform for very short (< 5 orbits) NR simulations.

The other key assumption, the presence of exact high frequency data, must also be put into the correct perspective. Not only do we say that the error of the NR part of the wave is negligible (an assumption that could easily be dropped if the NR mismatch becomes significant) we also use waveform families that directly resemble PN/NR hybrids. In other words, the additional error that is introduced in the phenomenological fitting and interpolation process is not taken into account here. Again, this is an error that can be quantified separately, but it has to be taken into account when interpreting the comparison of different complete waveform models, as was done in [45]. We merely state the fact here that *in principle* PN+NR combinations constitute sufficiently accurate target waveforms for the construction of template families.

This work can be complemented in many different ways. One obvious, yet involved extension is the completion of the parameter space by allowing arbitrary spin orientations that cause additional precession dynamics. Some steps towards building such hybrids have been taken place already [67, 68], but a deeper understanding of the waveform structure has to be gained before an extensive error analysis like the present one can be performed. Similarly, this study was restricted to the dominant spherical harmonic mode as it is crucial to understand and quantify the errors here first. Nevertheless, a final

waveform model would have to include higher modes as well, and the algorithm we presented should be easily adaptable to these cases.

Implementing more PN approximants and repeating our analysis with pairwise comparisons of various flavors of PN and EOB will help to fully understand the spread of equivalent descriptions of the inspiral process. When more contributions to PN expansions become available the present analysis has to be repeated, hopefully reflecting the enhanced knowledge of the analytical approximation. This is especially true for spinning binaries, where calculations of higher-order PN contributions are expected in the next few years.

Also, work is already underway [59] to extend previous work [58] and relate the parameter uncertainties found in this study to statistical errors that are inevitably present for signals with a given SNR in the detector. Only these results will allow for statements about how useful current waveform constructions are for parameter estimation and if the uncertainty in recovered parameters is dominated by the detector noise or the waveform model itself.

Finally and most interestingly, one should address the question of what kind of physics can be achieved given a certain performance of complete waveform models and, of course, given real GW detections with the upcoming generation of interferometers. It will be particularly important to analyze whether a certain disagreement between signal and model can be entirely explained by model uncertainties or if possibly unknown physical effects are the cause. This study serves as a first step to prepare for those kinds of questions.

ACKNOWLEDGMENTS

It is a pleasure to thank P. Ajith, S. Babak, B. Krishnan, F. Pannarale and E. Robinson for useful discussions. F. Ohme thanks Cardiff University for hospitality while some of this work was carried out. This work was supported in part by the DLR (Deutsches Zentrum für Luft-und Raumfahrt) and the IMPRS for Gravitational Wave Astronomy. M. Hannam was supported by FWF grant M1178 and Science and Technology Facilities Council grants ST/H008438/1 and ST/I001085/1. S. Husa was supported by DAAD grant D/07/13385 and grants FPA-2007-60220 and FPA-2010-16495 from the Spanish Ministry of Science, and the Spanish MICINN's Consolider-Genio 2010 Programme under grant MultiDark CSD2009-00064.

-
- [1] B. Sathyaprakash and B. Schutz, *Living Rev. Rel.*, **12**, 2 (2009), arXiv:0903.0338 [gr-qc].
 - [2] C. W. Helstrom, *Elements of signal detection and estimation* (Prentice-Hall, Inc., Upper Saddle River, NJ, USA, 1995) ISBN 0-13-808940-X.
 - [3] L. Blanchet, *Living Reviews in Relativity*, **9** (2006).
 - [4] C. Cutler *et al.*, *Phys. Rev. Lett.*, **70**, 2984 (1993), arXiv:astro-ph/9208005.
 - [5] T. Damour, B. R. Iyer, and B. S. Sathyaprakash, *Phys. Rev.*, **D57**, 885 (1998), arXiv:gr-qc/9708034.
 - [6] A. Buonanno, Y. Chen, and T. Damour, *Phys. Rev.*, **D74**, 104005 (2006), arXiv:gr-qc/0508067.
 - [7] M. Boyle *et al.*, *Phys. Rev.*, **D76**, 124038 (2007), arXiv:0710.0158 [gr-qc].
 - [8] A. Buonanno, B. Iyer, E. Ochsner, Y. Pan, and B. S. Sathyaprakash, *Phys. Rev.*, **D80**, 084043 (2009),

- arXiv:0907.0700 [gr-qc].
- [9] T. Damour, B. R. Iyer, and B. S. Sathyaprakash, *Phys. Rev.*, **D63**, 044023 (2001), arXiv:gr-qc/0010009.
- [10] T. Damour, B. R. Iyer, and B. S. Sathyaprakash, *Phys. Rev.*, **D66**, 027502 (2002), arXiv:gr-qc/0207021.
- [11] T. Damour, B. R. Iyer, and B. S. Sathyaprakash, *Phys. Rev.*, **D72**, 029901 (2005).
- [12] K. G. Arun, B. R. Iyer, B. S. Sathyaprakash, and P. A. Sundararajan, *Phys. Rev.*, **D71**, 084008 (2005), arXiv:gr-qc/0411146.
- [13] A. Gopakumar, (2007), arXiv:0712.3236 [gr-qc].
- [14] M. Hannam, S. Husa, B. Brügmann, and A. Gopakumar, *Phys. Rev.*, **D78**, 104007 (2008), arXiv:0712.3787 [gr-qc].
- [15] A. Buonanno and T. Damour, *Phys. Rev.*, **D59**, 084006 (1999), arXiv:gr-qc/9811091.
- [16] A. Buonanno and T. Damour, *Phys. Rev.*, **D62**, 064015 (2000), arXiv:gr-qc/0001013.
- [17] T. Damour, P. Jaranowski, and G. Schäfer, *Phys. Rev.*, **D62**, 084011 (2000), arXiv:gr-qc/0005034.
- [18] F. Pretorius, *Phys. Rev. Lett.*, **95**, 121101 (2005), arXiv:gr-qc/0507014.
- [19] M. Campanelli, C. O. Lousto, P. Marronetti, and Y. Zlochower, *Phys. Rev. Lett.*, **96**, 111101 (2006), arXiv:gr-qc/0511048.
- [20] J. G. Baker, J. Centrella, D.-I. Choi, M. Koppitz, and J. van Meter, *Phys. Rev. Lett.*, **96**, 111102 (2006), arXiv:gr-qc/0511103.
- [21] M. Hannam *et al.*, *Phys. Rev.*, **D79**, 084025 (2009), arXiv:0901.2437 [gr-qc].
- [22] M. Hannam, *Class. Quant. Grav.*, **26**, 114001 (2009), arXiv:0901.2931 [gr-qc].
- [23] I. Hinder, *Class. Quant. Grav.*, **27**, 114004 (2010), arXiv:1001.5161 [gr-qc].
- [24] J. M. Centrella, J. G. Baker, B. J. Kelly, and J. R. van Meter, *Ann.Rev.Nucl.Part.Sci.*, **60**, 75 (2010), arXiv:1010.2165 [gr-qc].
- [25] S. T. McWilliams, (2010), arXiv:1012.2872 [gr-qc].
- [26] T. Hinderer, B. D. Lackey, R. N. Lang, and J. S. Read, *Phys.Rev.*, **D81**, 123016 (2010), arXiv:0911.3535 [astro-ph.HE].
- [27] F. Pannarale, L. Rezzolla, F. Ohme, and J. S. Read, (2011), arXiv:1103.3526 [astro-ph.HE].
- [28] B. Abbott *et al.* (LIGO Scientific Collaboration), *Rept.Prog.Phys.*, **72**, 076901 (2009), arXiv:0711.3041 [gr-qc].
- [29] A. Buonanno *et al.*, *Phys. Rev.*, **D76**, 104049 (2007), arXiv:0706.3732 [gr-qc].
- [30] A. Buonanno *et al.*, *Phys. Rev.*, **D79**, 124028 (2009), arXiv:0902.0790 [gr-qc].
- [31] T. Damour, A. Nagar, E. N. Dorband, D. Pollney, and L. Rezzolla, *Phys. Rev.*, **D77**, 084017 (2008), arXiv:0712.3003 [gr-qc].
- [32] T. Damour, A. Nagar, M. Hannam, S. Husa, and B. Brügmann, *Phys. Rev.*, **D78**, 044039 (2008), arXiv:0803.3162 [gr-qc].
- [33] T. Damour and A. Nagar, *Phys. Rev.*, **D79**, 081503 (2009), arXiv:0902.0136 [gr-qc].
- [34] Y. Pan *et al.*, *Phys. Rev.*, **D81**, 084041 (2010), arXiv:0912.3466 [gr-qc].
- [35] N. Yunes, A. Buonanno, S. A. Hughes, M. Coleman Miller, and Y. Pan, *Phys. Rev. Lett.*, **104**, 091102 (2010), arXiv:0909.4263 [gr-qc].
- [36] Y. Pan, A. Buonanno, M. Boyle, L. T. Buchman, L. E. Kidder, *et al.*, (2011), arXiv:1106.1021 [gr-qc].
- [37] R. Sturani *et al.*, *J. Phys. Conf. Ser.*, **243**, 012007 (2010), arXiv:1005.0551 [gr-qc].
- [38] P. Ajith *et al.*, *Class. Quant. Grav.*, **24**, S689 (2007), arXiv:0704.3764 [gr-qc].
- [39] P. Ajith *et al.*, *Phys. Rev.*, **D77**, 104017 (2008), arXiv:0710.2335 [gr-qc].
- [40] P. Ajith *et al.*, *Phys. Rev. Lett.*, **106**, 241101 (2011), arXiv:0909.2867 [gr-qc].
- [41] L. Santamaría *et al.*, *Phys. Rev.*, **D82**, 064016 (2010), arXiv:1005.3306 [gr-qc].
- [42] M. Hannam, S. Husa, F. Ohme, and P. Ajith, *Phys.Rev.*, **D82**, 124052 (2010), arXiv:1008.2961 [gr-qc].
- [43] I. MacDonald, S. Nissanke, H. P. Pfeiffer, and H. P. Pfeiffer, *Class.Quant.Grav.*, **28**, 134002 (2011), arXiv:1102.5128 [gr-qc].
- [44] M. Boyle, (2011), arXiv:1103.5088 [gr-qc].
- [45] T. Damour, A. Nagar, and M. Trias, *Phys.Rev.*, **D83**, 024006 (2011), arXiv:1009.5998 [gr-qc].
- [46] L. Lindblom, B. J. Owen, and D. A. Brown, *Phys. Rev.*, **D78**, 124020 (2008), arXiv:0809.3844 [gr-qc].
- [47] L. Lindblom, *Phys.Rev.*, **D80**, 064019 (2009), arXiv:0907.0457 [gr-qc].
- [48] S. T. McWilliams, B. J. Kelly, and J. G. Baker, *Phys.Rev.*, **D82**, 024014 (2010), arXiv:1004.0961 [gr-qc].
- [49] E. Berti, V. Cardoso, J. A. González, U. Sperhake, and B. Brügmann, *Class. Quant. Grav.*, **25**, 114035 (2008), arXiv:0711.1097 [gr-qc].
- [50] L. Blanchet, G. Faye, B. R. Iyer, and S. Sinha, *Class. and Quant. Grav.*, **25**, 165003 (2008), arXiv:0802.1249 [gr-qc].
- [51] K. G. Arun, A. Buonanno, G. Faye, and E. Ochsner, *Phys. Rev.*, **D79**, 104023 (2009), arXiv:0810.5336 [gr-qc].
- [52] M. A. Scheel *et al.*, *Phys. Rev.*, **D79**, 024003 (2009), arXiv:0810.1767 [gr-qc].
- [53] Waveforms are available at <http://www.black-holes.org/Waveforms.html>.
- [54] P. Ajith *et al.*, (2007), arXiv:0709.0093 [gr-qc].
- [55] B. Vaishnav, I. Hinder, F. Herrmann, and D. Shoemaker, *Phys. Rev.*, **D76**, 084020 (2007), arXiv:0705.3829 [gr-qc].
- [56] C. Reisswig *et al.*, *Phys. Rev.*, **D80**, 124026 (2009), arXiv:0907.0462 [gr-qc].
- [57] M. Hannam, S. Husa, F. Ohme, D. Müller, and B. Brügmann, *Phys.Rev.*, **D82**, 124008 (2010), arXiv:1007.4789 [gr-qc].
- [58] P. Ajith and S. Bose, *Phys.Rev.*, **D79**, 084032 (2009), arXiv:0901.4936 [gr-qc].
- [59] E. Robinson, (2011), in preparation.
- [60] D. M. Gelino and T. E. Harrison, *Astrophys.J.*, **599**, 1254 (2003), arXiv:astro-ph/0308490 [astro-ph].
- [61] K. Belczynski, V. Kalogera, and T. Bulik, *Astrophys.J.*, **572**, 407 (2001), arXiv:astro-ph/0111452 [astro-ph].
- [62] M. Shibata, K. Kyutoku, T. Yamamoto, and K. Taniguchi, *Phys.Rev.*, **D79**, 044030 (2009), arXiv:0902.0416 [gr-qc].
- [63] J. Goussard, P. Haensel, and J. Zdukun, *Astron.Astrophys.*, **330**, 1005 (1998), arXiv:astro-ph/9711347 [astro-ph].
- [64] J. M. Lattimer and M. Prakash, *Phys.Rept.*, **442**, 109 (2007), arXiv:astro-ph/0612440 [astro-ph].
- [65] J. Hartung and J. Steinhoff, (2011), arXiv:1104.3079 [gr-qc].
- [66] A. Nagar, (2011), arXiv:1106.4349 [gr-qc].
- [67] M. Campanelli, C. O. Lousto, H. Nakano, and Y. Zlochower, *Phys.Rev.*, **D79**, 084010 (2009), arXiv:0808.0713 [gr-qc].
- [68] P. Schmidt, M. Hannam, S. Husa, and P. Ajith, (2010), arXiv:1012.2879 [gr-qc].